



Design and Optimization of Microstrip patch Antenna via Improved Metaheuristic Algorithm

Ramakrishna Guttula¹ · Venkateswara Rao Nandanavanam² · Vella Satyanarayana¹

Accepted: 13 April 2021 / Published online: 19 June 2021

© The Author(s), under exclusive licence to Springer Science+Business Media, LLC, part of Springer Nature 2021

Abstract

Nowadays, Microstrip patch antennas (MPA) are commonly deployed in various applications as it has number of benefits like compatibility, lower volume, low weight, low cost and easiness to install on rigid surfaces. However, MPA is restricted with narrow bandwidth and therefore, the enhancement of bandwidth is essential for the broad banded appliances. This work intends to develop a new approach, which derives a non-linear objective model to assist in designing the solution spaces of antenna constraints. For this, a new improved optimization concept termed as Elephant Herding Optimization with New Scaling Factor (EHO-NSF) is proposed that tunes the MPA parameters. The significance of the proposed work is to increase the antenna gain by optimally selecting the width, patch length, dielectric value of substrate, and substrate thickness of MPA. Eventually, analysis is carried out that validates the adopted model regarding gain, cost and efficiency analysis.

Keywords MPA · Bandwidth · Dielectric constant · Gain · EHO-NSF algorithm

Abbreviations

AA	Artificial Bee Colony-Based Antenna Design
CI	Characteristic Impedance
EMF	Electromagnetic Field
EHAD	Elephant Herding Based Antenna Design
EHF	Extremely High Frequency
ERI	Effective Refractive Index
FR4	Fire Resistant 4
FEM	Finite Element Method
FAD	Firefly-based AD
FAR	Field Asymmetry Ratio
GAD	Genetic-based AD
GWAD	Grey Wolf based AD
LAD	Lion Based AD
MIS	Modified-I-Shaped

✉ Ramakrishna Guttula
grkjosh643@gmail.com

¹ Aditya College of Engineering, Surampalem, Andhra Pradesh 533437, India

² Bapatla Engineering College, Bapatla, Andhra Pradesh 522101, India

MPA	Microstrip Patch Antenna
MTM	Metamaterials
MP-LAD	MP-LA-based AD
NPS	Non-Point-Symmetric
PS	Point-Symmetric
PSAD	Particle Swarm -Based AD
PGWAD	Proposed GWAD
RMPA	Rectangular Microstrip Patch Antenna
WOAD	Antenna Design Without Optimization

1 Introduction

The integrating ability of the MPA makes it more famous and constructive for appliances such as mobile, satellite or aerospace systems [1, 2]. Along with the striking characteristics like low-profile, light-weight, low-cost, and low-power, the realistic usage of MPA is restricted due to its narrow-band features, particularly in broad banded appliances [3, 4]. Improvement of MPA bandwidth is a key area of analysis for the past few decades. Various analyses are reported by means of diverse antenna geometry. Bandwidth improvements of patch antennas can be attained by a thicker substrate with lower permittivity; however radiation efficiency gets degraded because of the surface waves [5, 6, 7, 8].

Accordingly, MPAs are fed by the several techniques. These techniques are categorized into 2 types; “(a) contacting and (b) non-contacting”. As per the contact technique, the RF power is provided to radiation patch directly via a micro strip line [9, 10]. As per the non-contacting technique, EMF coupling is carried out for transferring the power among the radiating patch and micro strip line [11, 12]. The four well known feeding models are “the microstrip line, coaxial probe (both contacting schemes), aperture coupling and proximity coupling (both non-contacting schemes)”; however their patterns get vary with respect to frequency due to the false radiations. Moreover, they exhibit poor cross-polarization and back-radiation features [13, 14, 15].

Generally, the most renowned schemes for analysing MPA are the full wave model, transmit line and cavity models [16]. The full-wave scheme is very versatile, accurate and it treats the infinite and finite arrays, single elements, arbitrary elements, coupling, and stacked elements [17, 18]. The transmission line scheme is simpler and it offers better physical insights; however it is less precise. The cavity scheme offers good physical insight and is highly accurate; nevertheless it is complicated in nature.

The contributions of the work is given below.

1. Proposed a new algorithm termed as Elephant Herding Optimization with New Scaling Factor for fine-tuning the MPA parameters such as width, patch length, value of dielectric substrate, and substrate thickness for antenna gain enhancement.

The paper is arranged as: Section II portrays the review. Section III describe the modelling of MPA and section IV portrays the optimization of constraints of MPA design via Elephant Herding Optimization with New Scaling Factor. Section V and VI illustrates the outcomes and conclusion.

2 Literature Review

2.1 Related Works

In 2020, Dutta et al. [19] developed a RMPA with miniaturized and simple design with enhanced cross-polarization (XP) purity. The modelled scheme was highly flexible for tuning the antenna frequency for optimal performance. In addition, a comprehensive design was offered for estimating the resonance frequency of antenna and also for evaluating the respective resonant modes. Finally, the results obtained from the simulation have demonstrated the effectiveness of adopted concept.

In 2018, Qian et al. [20] have presented a new MPA design with narrow half-power beam-width and higher radiation gain loaded with MIS-MTM. Accordingly, a mathematical model was formulated for computing MPA in step by step procedure that aided in optimizing the constraints for optimal performance. This technique has also offered significant control for modelling the efficient transmitting antenna system in microwave appliances.

In 2020, Chandrashekar et al. [21] have presented a compact design of MPA for realizing the wideband features. Here, the annular metal-ring was deployed as superstrate and it was provided as inductive load to rectangular patch. In addition, the robust systematic method was exploited for choosing the size of ring and patch, in which they resonate closer to one another. This tactical model has ensured a wider harmonizing bandwidth with broader radiation. At last, the simulated results have revealed the enhancement of presented approach in terms of bandwidth.

In 2020, Rashmitha et al. [22] have designed and simulated a MPA that was well-suited for 5G communications. Here, the antenna worked at EHF ranges at 43.7 GHz. Accordingly, FR4 epoxy substrate was deployed in this work, and the antenna was examined for its radiation pattern, VSWR, return loss, distribution of current and gain. At last, the attained outcomes were confirmed and were examined for different appliances.

In 2019, Hocini et al. [23] have analyzed and designed the 5 terahertz MPA depending on “modified photonic band gap substrate” with a frequency of 0.5 to 0.8 THz. Consequently, the intention was to accomplish the optimal antenna features nearer to 0.65 THz that included appliances in communication and sensing fields. Moreover, the simulation was carried out on the basis of diverse substrates, together with aperiodic and periodic homogeneous photonic crystal substrates.

In 2021, Susamay et al. [24] have developed a novel quantitative constraint that has identified the most important factor for suitable geometry election of MPA, which could be applied in lower XP appliances. The importance of NPS and PS geometries was examined based on FAR, a novel constraint that quantified the level of electric field irregularities in MPA. From the experimentation, it was found that the adopted model could ensure low XP radiation.

In 2019, Shalini et al. [25] have proposed a “microstrip fed graphene based dual-polarized patch antenna that included single graphene patch fed by dual ports oriented orthogonally”. This port has provided the horizontal and vertical radiations in its relevant port directions. Moreover, the patch has a frequency of 3.98 THz and it was mounted on silicon substrate. Finally, the simulations were carried out, and the supremacy of the presented scheme was validated in terms of peak gain, return loss and efficiency.

In 2019, Hossein et al. [26] established MPA model for terahertz appliances. The adopted antenna has obtained minimal cost as the substrate was FR-4 and it has included higher radiation efficiency. On deploying the fractal structure, the radiation length of

present paths was raised and the antenna size was minimized. Finally, the results obtained from the simulation have revealed the efficacy of the modelled approach in terms of gain, efficiency and cost.

2.2 Review

Table 1 symbolizes the reviews on existing MPA design models. Cross-polarization [19] reveals improved gain and reduced polarization levels. However, there was degraded impedance matching. In addition, FEM exploited in [20] have offered high efficiency and increased gain efficiency, but it should consider more on radiation gain. Microstrip feeding technique [21] has effective control of Cross-polarization and attains efficient gain. However it needs consideration on radiation and band width properties. Trial and error method was deployed in [22] offered reduced impedance and high gain, but, there was implementation on real platforms. Finite integration technique [23] offers high radiation efficiency and reduced return loss. But, shock waves may degrade the performance of antenna. FAR [24] reduces cross-polarization and provides higher radiation efficiency. Yet, it requires consideration on varied types of feeding mechanisms. Dual-polarization based model [25] guarantees higher peak gain with minimal return loss. Nevertheless, it should consider more on polarization issues. FEM developed in [26] offers higher gain and minimized cost, but return loss should be focused more.

3 Modelling of Microstrip Patch Antenna

Figure 1 reveals the mechanism of radiation in MPA. Patch antennas usually include a ground plane and controlling patch. A dielectric media known as substrate is present at the centre of the design, which shows the exact value termed as dielectric constant. In general, patch sizes are said to be smaller than the ground and substrate, the. While designing a MPA, a resonance frequency and dielectric medium are chosen based on the size of MPA. In addition, the dielectric substrates with minimal dielectric constant are required for enhancing the antenna performances, wherein the efficiency is improved with higher radiation and bandwidths.

The noteworthy constraints while designing the MPA is depicted below.

Width computation Eq. (1) shows the width evaluation of MPA, wherein, r^f points out the resonant frequency, ϵ_r points out the value of dielectric substrate and L points out light speed. Equation (2) portrays the formulation for r^f , wherein ϵ^{re} points out the effective refractive index and P points out patch length [27].

$$W = \frac{L}{2r^f} \sqrt{\frac{2}{\epsilon_r + 1}} \quad (1)$$

$$r^f = \frac{L}{2P\sqrt{\epsilon^{re}}} \quad (2)$$

Height assessment The height (H) of MPA is computed as given in Eq. (3), wherein T points out thickness of substrate [27].

Table 1 Reviews on traditional MPA designs

Author	Method	Features	Challenges
Dutta et al. [19]	Cross-polarization	Enhanced peak gain Minimal polarization levels	Degraded impedance matching
Tian et al. [20]	FEM model	High efficiency Increased gain efficiency	Should consider more on radiation gain
Chandrashekar et al. [21]	Microstrip feeding technique	Minimal Cross-polarization Attains high gain	Need consideration on radiation and band width properties
Rashmitha et al. [22]	Trial and error method	High gain Reduced impedance	No implementation on real platforms
Hocini et al. [23]	Finite integration technique	High radiation efficiency Reduced return loss	Shock waves may degrade the performance of antenna
Susamay et al. [24]	FAR	Minimal Cross-polarization High radiation efficiency	Requires consideration on varied types of feeding mechanisms Should focus more on XP performance
Shalini et al. [25]	Dual-polarization based model	Higher peak gain Minimal return loss	Should consider more on polarization issues
Hossein <i>et al</i> [26]	FEM model	Minimal cost Higher gain	Return loss should be focused more

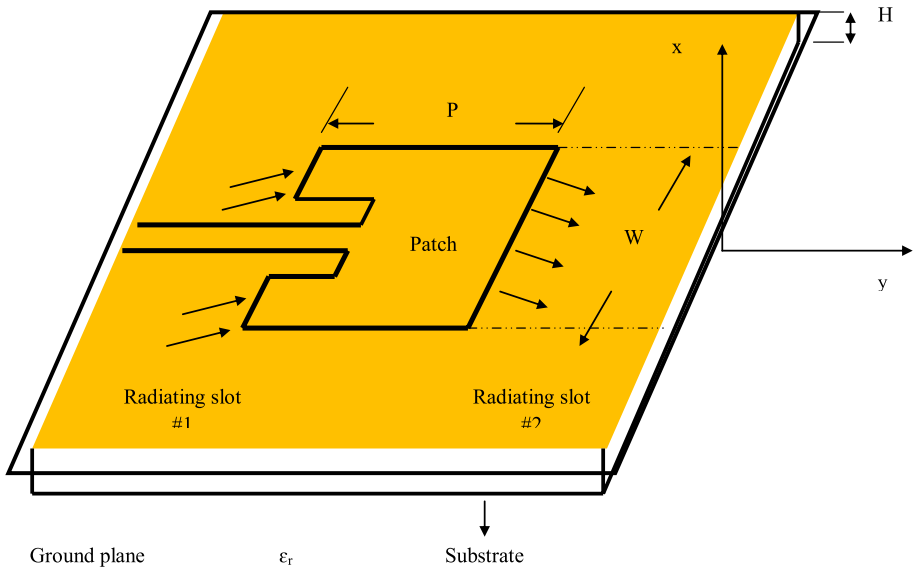


Fig. 1 Radiation pattern for MPA design

$$H = \frac{T}{1000 \times 2.54} \tag{3}$$

ERI assessment The constraint, ϵ^{re} is evaluated as per the Eq. (4), wherein H points out the substrate’s height.

$$\epsilon^{re} = \frac{\epsilon_r + 1}{2} + \frac{\epsilon_r + 1}{2} \left[1 + 12 \frac{H}{W} \right]^{-1/2}, \frac{W}{H} > 1 \tag{4}$$

Normalized length assessment The MPA’s normalized length (ΔP) is evaluated as per Eq. (5).

$$\frac{\Delta P}{H} = 0.412 \frac{(\epsilon^{re} + 0.3) \left(\frac{W}{H} + 0.264 \right)}{(\epsilon^{re} - 0.258) \left(\frac{W}{H} + 0.8 \right)} \tag{5}$$

Length assessment The length of MPA indicated by (P) is evaluated as per Eq. (6).

$$P = \frac{L}{2r^f \sqrt{\epsilon^{re}}} - 2\Delta P \tag{6}$$

CI calculation Eq. (7) demonstrates the CI of transition element, wherein, Y_i points out the patch impedance and is evaluated as per Eq. (8) [27].

$$Y_i = \sqrt{50 + Z_i} \tag{7}$$

$$Y_i = 90 \frac{\epsilon_r^2}{\epsilon_r - 1} \left(\frac{P}{W} \right)^2 \quad (8)$$

Gain computation The proportion of antenna intensity to the input power constitutes the MPA gain. Equation (9) defines the MPA gain, where I indicates the input antenna power and R_I points out radiation intensity [27].

$$M_A = 4\pi \left(\frac{R_I}{I} \right) \quad (9)$$

4 Optimized MPA Design via Improved Elephant Herding Optimization

4.1 Objective Model and Solution Encoding

The adopted scheme intends to increase the antenna gain as defined in Eq. (10). Accordingly, the design parameters like P, W, T and ϵ_r of MPA are optimally tuned by the EHO-NSF. The input solution to adopted algorithm is revealed in Fig. 2.

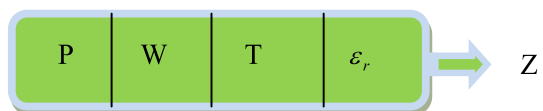
$$M_A^* = \arg \max_{(P, W, T, \epsilon_r)} (M_A) \quad (10)$$

4.2 Proposed EHO-NSF Algorithm

The existing EHO model [28] shows better convergence and resolves varied optimization issues, nevertheless, to improve the searching quality, certain modifications are needed and this work introduces a modified version with new scaling factor. In general, self-improvement is proven to be promising in traditional optimization algorithms [29, 30, 31, 32, 33, 34, 35, 36]. The procedure of proposed EHO-NSF model is as follows: Elephants are societal creatures that survive in social groups including calves and females. The group involves various clans, and each clan is headed by a matriarch. Usually, female elephants live with the clans, whereas the male elephants leave the clans when they grow up. The following assumptions are considered in EHO-NSF.

1. The population includes several clans and every clan comprises of female and male elephants.
2. Some of the male elephants leaves the clan and live alone
3. Each clan is headed by a matriarch.

Fig. 2 Solution encoding



Clan-updating Operator As per the nature of the elephants, the elephants in a clan are lead by matriarch. Thus, the matriarch c has a major impact on the novel positions of all elephants. The elephant j in clan c is updated by Eq. (11), here $Z_{c,j}$ and $Z_{n,c,j}$ points out the old position and new position of elephant j in clan c , correspondingly. $Z_{best,c}$ is matriarch c that indicates the best elephant in clan c . Conventionally, the scale factor α lies between 0 and 1. As per the presented model, α is computed as shown in Eq. (12), where K denotes the elitism parameter (that indicates how many best elephants to move from one generation to next generation) and Z_{best} refers to best fitness at each iteration.

$$Z_{n,c,j} = Z_{c,j} + \alpha \cdot r \cdot (Z_{best,c} - Z_{c,j}) \quad (11)$$

$$\alpha = (j/K) * Z_{best} \quad (12)$$

However, the best elephant in each clan could not be updated as per Eq. (11). As per the developed model, it can be updated as per Eq. (13), where CL points out the chromosome length and ran points out the random integer.

$$Z_{n,c,j} = \text{round}(1 + (CL - 1)) \times ran \quad (13)$$

4.3 Separating Operator

The separating procedure, in which the male elephants depart their family group is modelled into separating operator. The separating operator is computed based on the worst fitness as shown in Eq. (14), where Z_{\min} and Z_{\max} are the minimum and maximum bounds of positions correspondingly. $Z_{worst,c}$ indicate the worst elephant individual of clan c and r represents the random integer between 0 and 1. Algorithm 1 reveals the pseudo code of the presented EHO-NSF model.

$$Z_{worst,c} = Z_{\min} + r \cdot (Z_{\max} - Z_{\min} + 1) \quad (14)$$

Algorithm 1: Implemented EHO-NSF method

Initialization

Compute the fitness as per Eq. (10)

Repeat

 Arrange all the elephants according to their fitness

 Clan updating

 For $c=1$ to $nclan$ (for each clans of elephant population) do

 For $j=1$ to nc (for every elephants in clan c) do

 If $Z_{c,j} = Z_{best,ci}$ then

 Update $Z_{c,j}$ and generate $Z_{n,c,j}$ by Eq. (13)

 Else

 Compute α as per Eq. (12)

 Update $Z_{c,j}$ and generate $Z_{n,c,j}$ by Eqn. (11)

 End if

 End for j

 End c

 Separating operator

 For $c=1$ to $nclan$ (for every clan of elephant population) do

 Replace the clan with worst elephant in by Eqn. (14)

 End for c

 Evaluate population by the newly update positions

 Until (Maximum number of generations)

5 Results and Discussions

5.1 Simulation Set Up

The adopted MPA design was simulated in MATLAB and the results were achieved. Here, the population size was assigned as 10 and the iteration count was assigned as 100. In addition, the superiority of the presented antenna model was validated by comparing it with other existing schemes like AAD [37], WOAD [38], FAD [39], LAD [40], GAD [41], GWAD [42], PGWAD [43], PSAD [44], EHAD [28] and MP-LAD [27]. In addition, the analysis was carried out with respect to gain, directivity, cost, CI and efficiency.

5.2 Performance Analysis

The performance of the adopted EHO-NSFAD model over existing models like AAD, WOAD, FAD, GAD, GWAD, PSAD, LAD, PGWAD, EHAD and MP-LAD is given in Fig. 3 for varied frequency levels that ranges from 77, 74, 72, 70, 68 and 65 GHz. Accordingly, the gain, directivity, CI, and efficiency are observed from Fig. 3(a) to (d) respectively. From the analysis, the presented model has attained better values for gain, directivity, CI, and efficiency when compared over the other existing models. Particularly, from Fig. 3(a), a higher gain of 17.2 dB has been attained by the EHO-NSFAD scheme, which is 8.14%, 5.23%, 23.26%, 23.26%, 5.23%, 12.79%, 8.14%, 23.26%, 5.23% and 1.16% superior to traditional AAD, WOAD, FAD, GAD, GWAD, PSAD, LAD, PGWAD, EHAD and MP-LAD models at 77 GHz. Also, the directivity analysis and CI analysis for the proposed EHO-NSF model over conventional schemes is given in Fig. 3(b) and (c) for varied frequency levels. Moreover, from Fig. 3(c), the CI attained by the adopted scheme is 10%, 14.67%, 22%, 14.67%, 10%, 6.67%, 10%, 3.33%, 10% and 3.33% superior to traditional AAD, WOAD, FAD, GAD, GWAD, PSAD, LAD, PGWAD, EHAD and MP-LAD models at a frequency of 70 GHz respectively. From the analysis, the adopted model is accomplished with higher directivity values, thus ensuring the superior performance of the work. Specifically, the directivity attained by the adopted scheme is 35.14%, 27.03%, 40.54%, 40.54%, 48.65%, 37.84%, 32.43%, 27.03%, 45.95% and 27.03% superior to traditional AAD,

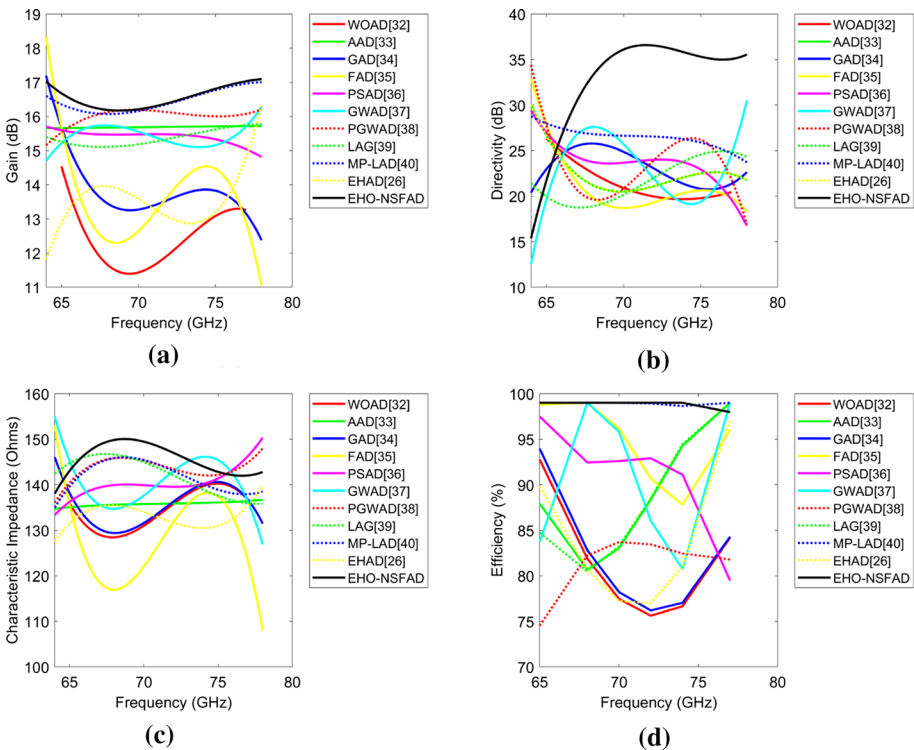


Fig. 3 Performance analysis of the developed scheme over traditional schemes in terms of (a) Gain (b) Directivity (c) CI (d) Efficiency

WOAD, FAD, GAD, GWAD, PSAD, LAD, PGWAD, EHAD and MP-LAD schemes at a frequency of 75 GHz respectively. Consequently, the overall examination of the developed model over existing models for varied design constraints is shown in Table 2. Thus, from the evaluation, it is clear that the presented EHO-NSFAD model has obtained improved performance when compared to the state-of-art techniques.

5.3 Analysis on Radiation Pattern

The radiation patterns of the MPA design attained by the proposed EHO-NSFAD model over existing schemes are illustrated in Fig. 4. Consequently, the radiation patterns are observed for diverse frequencies. In fact, a higher radiation pattern ensures the better performance of the system. On observing the graphs, the presented scheme has accomplished bigger side lobes as well as main lobe than the existing schemes. Particularly from Fig. 4(a), the side lobes as well as main lobe of adopted scheme at 65 GHz has revealed a higher radiation pattern when computed over existing schemes. Similarly, from Fig. 3(b)–(f), the developed EHO-NSFAD model has obtained amplified side lobes as well as main lobe whose sizes are higher over other conventional schemes for varied frequencies.

5.4 E-Plane Analysis

Usually, E-plane includes the capability to discover the orientation of the antenna radio waves. Accordingly, E-plane analysis is done by altering the frequencies at 77, 74, 72, 70, 68 and 65 GHz, where the DOA is assigned as 90°. A proficient antenna design can be accomplished only if the side lobes and main lobe attain maximal dimensions. From Fig. 5(a), the dimensions of side lobes and the main lobe offered by the developed EHO-NSFAD scheme at the frequency of 65 GHz is higher than the existing AAD, WOAD, FAD, GAD, GWAD, PSAD, LAD, PGWAD, EHAD and MP-LAD schemes. Moreover, at the frequency of 68 and 70 GHz, the sizes of side lobes as well as main lobe of presented EHO-NSFAD model are much bigger over the compared schemes. In the same way, the size of side lobes as well as main lobe of developed EHO-NSFAD model at diverse frequencies such as, 77, 74 and 72 GHz are found to expose higher radiation patterns than the conventional schemes.

Table 2 Overall analysis of developed model over traditional models

Methods	Directivity	Gain	CI	Efficiency
WOAD [38]	21.629	12.603	134.59	8142.8
AAD [37]	22.33	15.687	135.78	8889
GAD [41]	23.207	13.827	135.39	8208.5
FAD [39]	20.974	13.629	127.99	9505.7
PSAD [44]	23.605	15.411	140.35	9100.3
GWAD [42]	23.113	15.431	140.51	9129.4
PGWAD [43]	23.38	16.013	143.64	8135.7
LAD [40]	21.625	15.361	142.19	8871.9
MP-LAD [27]	26.477	16.428	141.99	9937.8
EHAD [28]	33.071	13.532	133.1	8381.6
EHO-NSFAD	22.096	16.53	145.9	9987.1

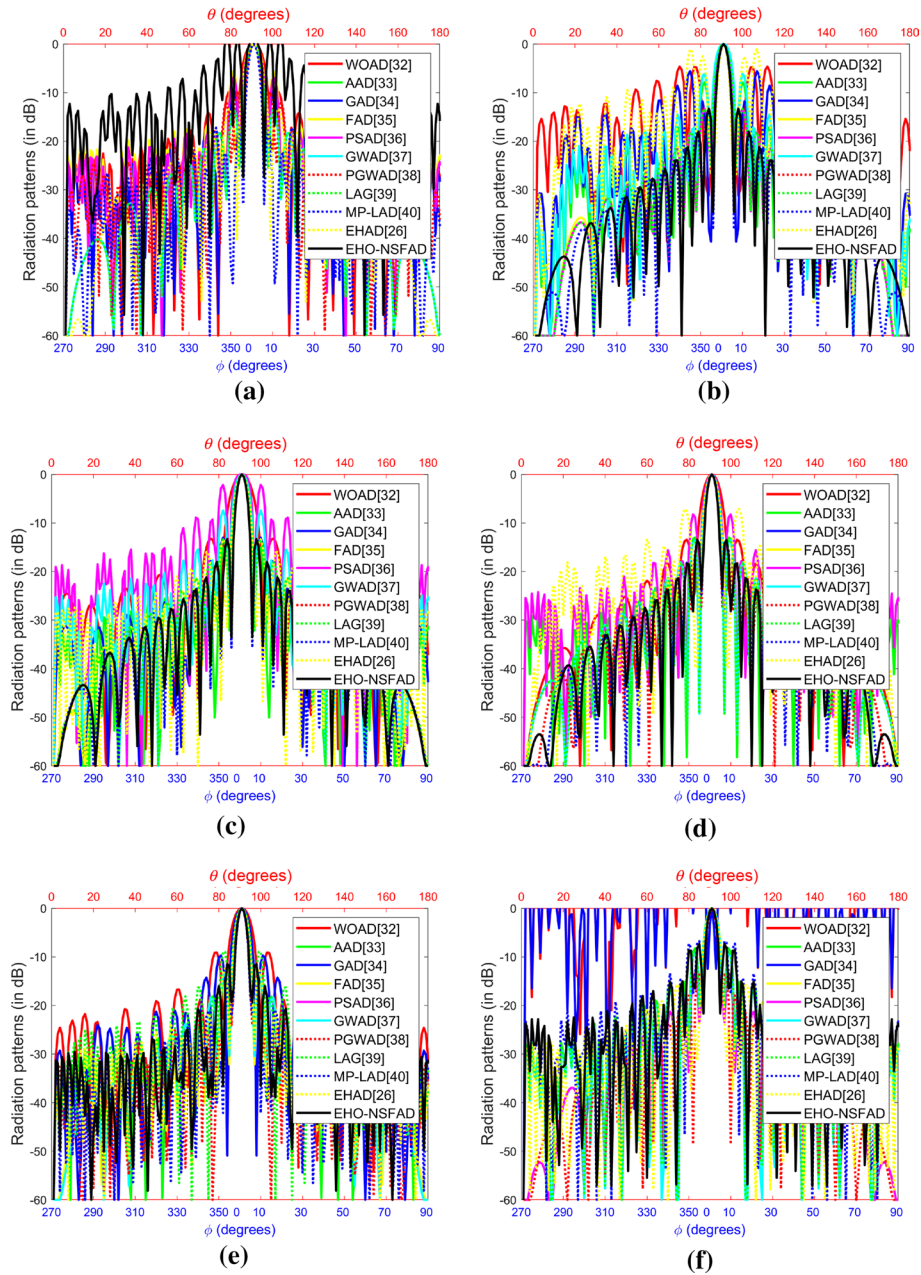


Fig. 4 Radiation pattern of the developed scheme over traditional schemes for varied frequencies like **a** 65 GHz, **b** 68 GHz, **c** 70 GHz, **d** 72 GHz, **e** 74 GHz and **f** 77 GHz

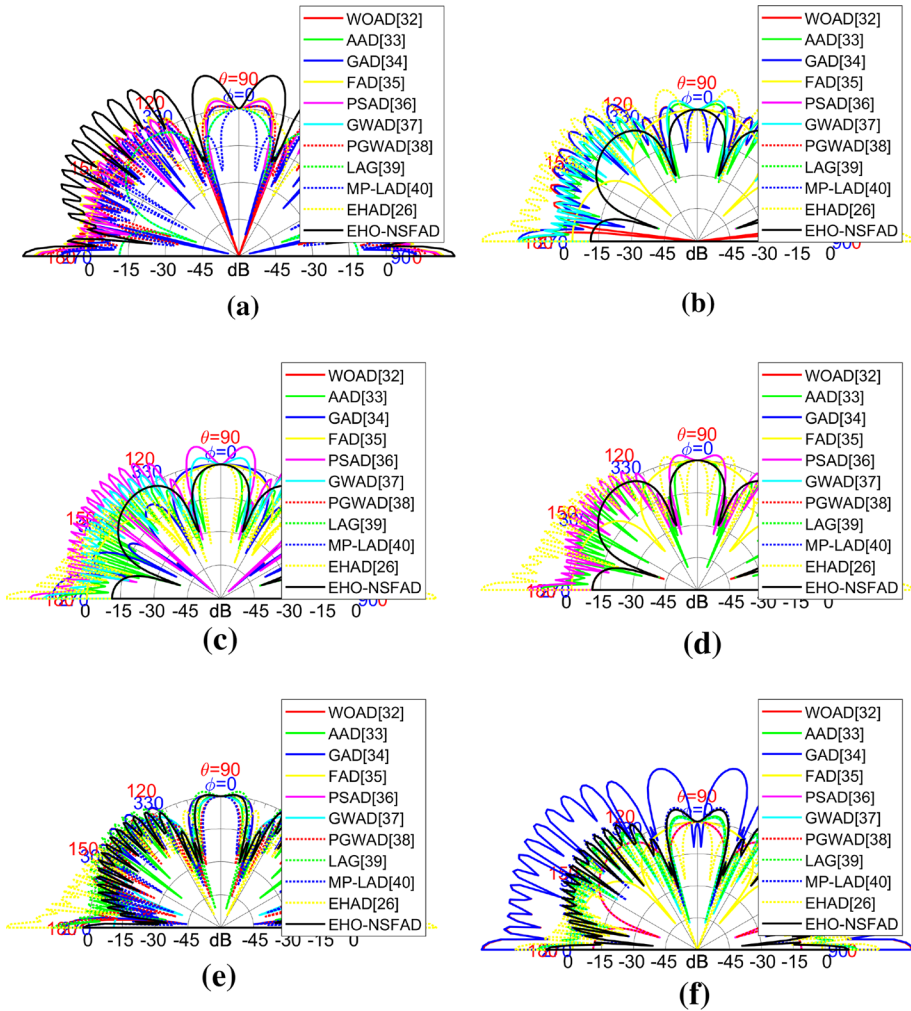


Fig. 5 E-plane analysis of developed scheme over traditional schemes for varied frequencies namely **a** 65 GHz, **b** 68 GHz, **c** 70 GHz, **d** 72 GHz, **e** 74 GHz and **f** 77 GHz

5.5 H-Plane Analysis

The analysis on H-plane attained by the developed EHO-NSFAD model over existing models at varied frequencies such as, 77, 74, 72, 70, 68 and 65 GHz is shown in Fig. 6. For all the frequencies, the sizes of main lobe and the side lobes of presented antenna model are amplified than the existing models. Thereby, the improvement of the developed EHO-NSFAD scheme in terms of H-plane is proved from the outcomes.

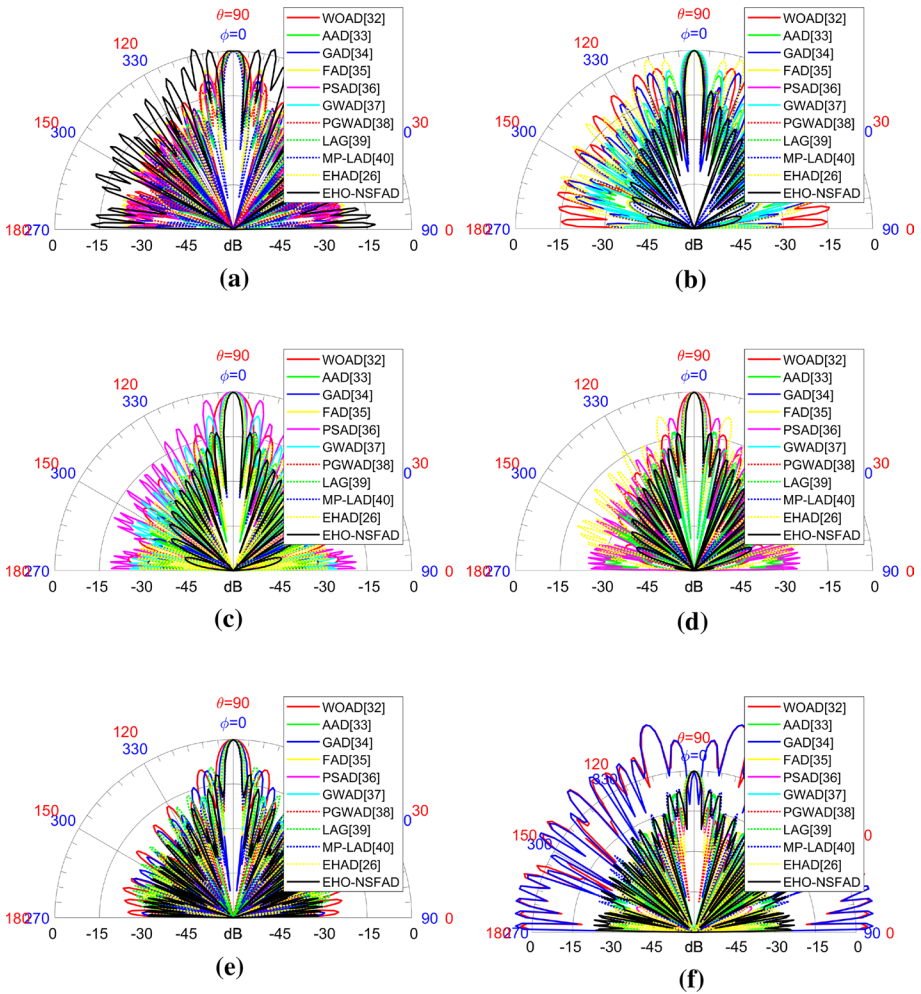


Fig. 6 H-plane analysis of developed scheme over traditional schemes for varied frequencies namely “a 65 GHz, b 68 GHz, c 70 GHz, d 72 GHz, e 74 GHz and f 77 GHz a 65 GHz, b 68 GHz, c 70 GHz, d 72 GHz, e 74 GHz and f 77 GHz”

5.6 Convergence Analysis

The convergence analysis (cost) of adopted scheme (EHO-NSFAD) over the existing schemes is shown in Fig. 7 for varied frequencies such as, 77, 74, 72, 70, 68 and 65 GHz. Here, cost is evaluated as: (cost=1/gain). Accordingly, the analysis is performed by varying the iterations from 0 to 100. On examining the outcomes, the cost values attained by the developed EHO-NSFAD model are found to be lower than the compared schemes for all frequencies. For instance, at 65 GHz, the proposed model at iteration 50 has attained a minimal cost value of 0.06, which is much lower when compared to other methods. That is, the adopted scheme is 6.67%, 11.67%, 6.67%, 6.67%, 11.67%, 6.67%, 11.67%, 5.83%, 30% and 5% superior to traditional AAD, WOAD, WOAD, AAD, GAD, FAD, PSAD, GWAD, PGWAD, LAG, MP-LAD, EHAD, and EHO-NSFAD, respectively.

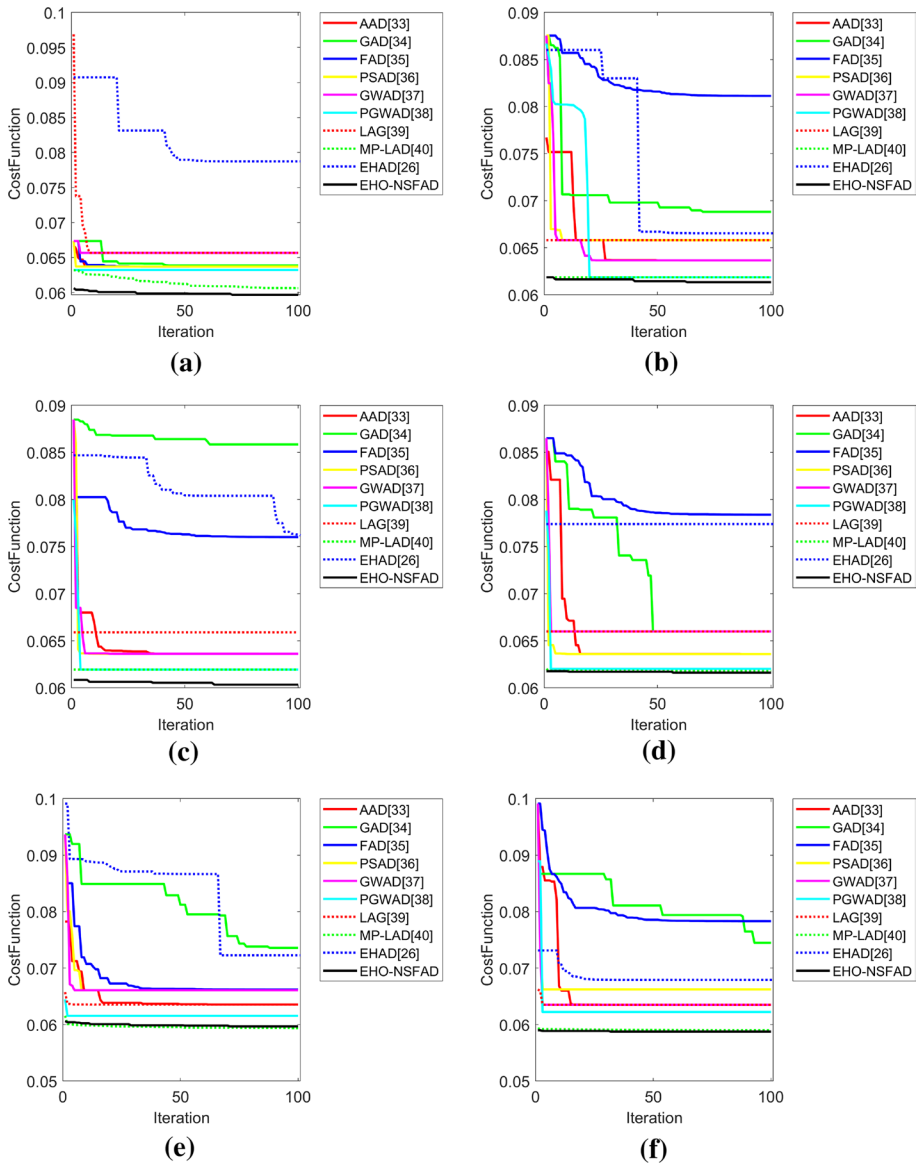


Fig. 7 Cost of for developed scheme over traditional schemes for varied frequencies namely **a** 65 GHz, **b** 68 GHz, **c** 70 GHz, **d** 72 GHz, **e** 74 GHz and **f** 77 GHz

FAD, GAD, GWAD, PSAD, LAD, PGWAD, EHAD and MP-LAD schemes. Thereby, the superiority of presented EHO-NSFAD method was validated.

The results are encouraging and they show better performance on the microstrip patch antenna. Further, based on the availability of the resources like hardware requirements this work will be further extended to experiment real-time.

6 Conclusion

This paper introduced a novel antenna design by integrating the EHO-NSFAD based optimization concept. Accordingly, the MPA parameters such as width, patch length, substrate thickness and dielectric substrate value were optimized by the presented EHO-NSFAD for attaining increased gain. Furthermore, analysis was carried out that proved the efficiency of the presented work. From the analysis, the adopted model was found to accomplish higher directivity values, thus ensuring the superior performance of the work. Specifically, the directivity attained by the adopted scheme was 35.14%, 27.03%, 40.54%, 40.54%, 48.65%, 37.84%, 32.43%, 27.03%, 45.95% and 27.03% superior to traditional AAD, WOAD, FAD, GAD, GWAD, PSAD, LAD, PGWAD, EHAD and MP-LAD schemes at a frequency of 75 GHz respectively. Thus, the effectiveness of the presented EHO-NSFAD method was proved via valuable analysis.

Author contributions Ramakrishna Guttula conceived the presented idea and designed the analysis. Also, he carried out the experiment and wrote the manuscript with support from Venkateswara Rao Nandanavanam and Vella Satyanarayana. All authors discussed the results and contributed to the final manuscript. All authors read and approved the final manuscript.

Funding Not applicable.

Availability of data and materials Not applicable.

Code availability Not applicable.

Declarations

Conflict of interest The authors declare that they have no conflict of interest.

References

1. Jain, S., Mishra, P. K., & Mishra, P. K. (2020). Design and analysis of moisture content of hevea latex rubber using microstrip patch antenna with DGS. *Materials Today: Proceedings Part 2*, 29, 556–560
2. Koziel, S., Ogurtsov, S., Zieniutycz, W., & Sorokosz, L. (2014). Expedited design of microstrip antenna subarrays using surrogate-based optimization. *IEEE Antennas and Wireless Propagation Letters*, 13, 635–638
3. Kushwaha, R. K., Karuppanan, P., & Malviya, L. D. (2018). Design and analysis of novel microstrip patch antenna on photonic crystal in THz. *Physica B: Condensed Matter*, 545, 107–112
4. Khandelwal, M. K., Kanaujia, B. K., Dwari, S., Kumar, S., & Gautam, A. K. (2014). Analysis and design of wide band Microstrip-line-fed antenna with defected ground structure for Ku band applications. *AEU-International Journal of Electronics and Communications*, 68(10), 951–957
5. Sharma, N., & Sharma, V. (2018). A design of Microstrip Patch Antenna using hybrid fractal slot for wideband applications. *Ain Shams Engineering Journal*, 9(4), 2491–2497
6. Prema, N., & Kumar, A. (2016). Design of multiband microstrip patch antenna for C and X band. *Optik*, 127(20), 8812–8818
7. Mathur, D., Bhatnagar, S. K., & Sahula, V. (2014). Quick estimation of rectangular patch antenna dimensions based on equivalent design concept. *IEEE Antennas and Wireless Propagation Letters*, 13, 1469–1472
8. Nejati, A., Sadeghzadeh, R. A., & Geran, F. (2014). Effect of photonic crystal and frequency selective surface implementation on gain enhancement in the microstrip patch antenna at terahertz frequency. *Physica B: Condensed Matter*, 449, 113–120

9. Yang, X., Geyi, W., & Sun, H. (2017). Optimum design of wireless power transmission system using microstrip patch antenna arrays. *IEEE Antennas and Wireless Propagation Letters*, *16*, 1824–1827
10. Bhongale, S. R., Ingavale, H. R., Shinde, T. J., & Vasambekar, P. N. (2018). Microwave sintered Mg-Cd ferrite substrates for microstrip patch antennas in X-band. *AEU-International Journal of Electronics and Communications*, *96*, 246–251
11. Singh, A., Mehra, R. M., & Pandey, V. K. (2020). Design and Optimization of Microstrip Patch Antenna for UWB Applications Using Moth-Flame Optimization Algorithm. *Wireless Personal Communications*, 1-18
12. Saxena, N. K., Kumar, N., & Pourush, P. K. S. (2015). Radiation characteristics of microstrip rectangular patch antenna fabricated on LiTiMg ferrite substrate. *AEU-International Journal of Electronics and Communications*, *69*(12), 1741–1744
13. Gupta, M. (2018). Vinita Mathur “Koch boundary on the square patch microstrip antenna for ultra wideband applications.” *Alexandria Engineering Journal*, *57*(3), 2113–2122
14. Emadeddin, A., Shad, S., Rahimian, Z., & Hassani, H. R. (2017). High mutual coupling reduction between microstrip patch antennas using novel structure. *AEU-International Journal of Electronics and Communications*, *71*, 152–156
15. Nuangpirom, P., Klinbumrung, K., Tangthong, N., & Akatimagool, S. (2016). Wave iterative computation for fractal microstrip patch antenna. *Procedia Computer Science*, *86*, 39–42
16. Anantha, B., Merugu, L., & Rao, P. S. (2017). A novel single feed frequency and polarization reconfigurable microstrip patch antenna. *AEU-International Journal of Electronics and communications*, *72*, 8–16
17. Naderi, M., & Zarrabi, F. B. (2018). Fereshteh Sadat Jafari, Speideh Ebrahimi, “Fractal EBG structure for shielding and reducing the mutual coupling in microstrip patch antenna array.” *AEU-International Journal of Electronics and Communications*, *93*, 261–267
18. Bharathi, A., Lakshminarayana, M., & Rao, P. S. (2017). A quad-polarization and frequency reconfigurable square ring slot loaded microstrip patch antenna for WLAN applications. *AEU-International Journal of Electronics and Communications*, *78*, 15–23
19. Poornima, S., Dutta, K., & Chandramma, S. (2020). Flexible and miniaturized design of microstrip patch antenna with improved cross-polarized radiation. *AEU-International Journal of Electronics and Communications*, *116*, 153083
20. Li, T. Q., Ma, B., & Lv, W. R. (2018). A novel design of microstrip patch antenna array with modified-I-shaped electromagnetic metamaterials applied in microwave wireless power transmission. *Optik*, *173*, 193–205
21. Chandrashekar, K. S., Dutta, K., Gajera, H., Poornima, S., & Chandramma, S. (2020). An analytical approach of designing compact microstrip patch antenna using metal-ring superstrate for wideband and broadside radiations. *AEU-International Journal of Electronics and Communications*, *127*, 153437
22. Rashmitha, R., Niran, N., Jugale, A. A., & Ahmed, M. R. (2020). Microstrip patch antenna design for fixed mobile and satellite 5G communications. *Procedia Computer Science*, *171*, 2073–2079
23. Hocini, A., Temmar, M. N., Khedrouche, D., & Zamani, M. (2019). Novel approach for the design and analysis of a terahertz microstrip patch antenna based on photonic crystals. *Photonics and Nanostructures-Fundamentals and Applications*, *36*: 100723
24. Samanta, S., Reddy, P. S., & Mandal, K. (2021). Field Asymmetry Ratio: A new quantitative parameter to select microstrip antenna geometries for low cross-polarization application. *AEU-International Journal of Electronics and Communications*, *128*, 153519
25. Shalini, M., & Madhan, M. G. (2019). Design and analysis of a dual-polarized graphene based microstrip patch antenna for terahertz applications. *Optik*, *194*, 163050
26. Davoudabadifarhani, H., & Ghalamkari, B. (2019). High efficiency miniaturized microstrip patch antenna for wideband terahertz communications applications. *Optik*, *194*, 163118
27. Guttula, R., & Nandanavanam, V. R. (2020). Mutation probability-based lion algorithm for design and optimization of microstrip patch antenna. *Evolutionary Intelligence*, *13*, 331–344. <https://doi.org/10.1007/s12065-019-00292-9>
28. Elhosseini, M. A., El Sehiemy, R. A., Rashwan, Y. I., & Gao, X. Z. (2019). On the performance improvement of elephant herding optimization algorithm. *Knowledge-Based Systems*, *166*, 58–70
29. Rajakumar, B. R. (2013). Impact of static and adaptive mutation techniques on genetic algorithm. *International Journal of Hybrid Intelligent Systems*, *10*(1), 11–22. <https://doi.org/10.3233/HIS-120161>

30. Rajakumar, B. R. (2013). Static and adaptive mutation techniques for genetic algorithm: A systematic comparative analysis. *International Journal of Computational Science and Engineering*, 8(2), 180–193. <https://doi.org/10.1504/IJCSE.2013.053087>
31. Swamy, S. M., Rajakumar, B. R. and Valarmathi, I. R. (2013) "Design of hybrid wind and photovoltaic power system using opposition-based genetic algorithm with cauchy mutation". IET Chennai Fourth International Conference on Sustainable Energy and Intelligent Systems (SEISCON 2013), Chennai, India <https://doi.org/10.1049/ic.2013.0361>.
32. George, A. and Rajakumar, B. R. (2013) "APOGA: An adaptive population pool size based genetic algorithm". AASRI Procedia-2013 AASRI Conference on Intelligent Systems and Control (ISC 2013), Vol. 4, (pp. 288–296) <https://doi.org/10.1016/j.aasri.2013.10.043>.
33. Rajakumar, B. R. and George, A. (2012) "A new adaptive mutation technique for genetic algorithm". In proceedings of IEEE International Conference on Computational Intelligence and Computing Research (ICCCIR), (pp. 1–7), 18–20, Coimbatore, India <https://doi.org/10.1109/ICCCIR.2012.6510293>.
34. Shelke, P. M., & Prasad, R. S. (2020). (2020), "Improved sine-cosine algorithm for anti forensics JPEG compression." *Multimedia Research*, 3(1), 33–44
35. Jagtap, A. M., & Gomathi, N. (2019). Improved salp swarm algorithm for network connectivity in mobile sensor network". *Journal of Networking and Communication Systems*, 2(3), 11–19
36. Poluru, R. K., & Kumar, R. L. (2019). Enhancement of ATC by optimizing TCSC configuration using adaptive moth flame optimization algorithm. *Journal of Computational Mechanics, Power System and Control*, 2(3), 1–9
37. Kiran, M. S., & Findik, O. (2015). A directed artificial bee colony algorithm. *Applied Soft Computing*, 26, 454–462
38. Sivia, J. S., Pharwaha, A. P. S., & Kamal, T. S. (2016). Neurocomputational models for parameter estimation of circular microstrip patch antennas. *Procedia Computer Science*, 85, 393–400
39. Fister, I., Fister, I., Yang, X.-S., & Brest, J. (2013). A comprehensive review of firefly algorithms. *Swarm and Evolutionary Computation*, 13, 34–46
40. Boothalingam, R. (2018). Optimization using lion algorithm: a biological inspiration from lion's social behavior. *Evolutionary Intelligence*, 11(1), 31–52
41. McCall, J. (2005). Genetic algorithms for modelling and optimisation. *Journal of Computational and APPLIED Mathematics*, 184(1), 205–222
42. Mirjalili, S., Mirjalili, S. M., & Lewis, A. (2014). Grey wolf optimizer. *Advances in Engineering Software*, 69, 46–61
43. Guttula, R., & Nandanavanam, V. R. (2020). Patch antenna design optimization using opposition based grey wolf optimizer and map-reduce framework. *Data Technologies and Applications*, 54(1), 103–120. <https://doi.org/10.1108/DTA-06-2019-0084>
44. Zhang, J., & Xia, P. (2017). An improved PSO algorithm for parameter identification of nonlinear dynamic hysteretic models. *Journal of Sound and Vibration*, 389, 153–167

Publisher's Note Springer Nature remains neutral with regard to jurisdictional claims in published maps and institutional affiliations.



Dr. Ramakrishna Guttula received his B. Tech in Electronics and Communication Engineering from Acharya Nagarjuna University, India and MTech in Instrumentation and Control Systems from JNTUK, India. He obtained his Ph.D. from Acharya Nagarjuna University, AP, India. His current research interest includes microstrip antennas, Electromagnetic field theory and Solid state electronics. Currently he is working as an Associate Professor in the Department of Electronics and Communication Engineering, Aditya College of Engineering, Surampalem, AP, India. He is a life member of IETE.



Dr. Venkateswara Rao Nandanavanam received B.Tech degree in Electronics and Communication Engineering from JNT University, Kakinada and ME from Osmania University. He received a PhD from JNTU, Hyderabad. Presently working as head and professor in the department of ECE, Bapatla engineering college, Bapatla, India. He has authored 43 papers in International/National journals and presented 20 International/National Conferences. His research areas are mainly in Satellite communication and Antennas. He is also interested in RF and Microwave.



Vella Satyanarayana received his B.Tech degree in Electronics and Communication Engineering from JNTU, Hyderabad and M.Tech degree in VLSI Design from JNTUK, Andhra Pradesh, India. He is a life member of IETE. Currently pursuing Ph.D. from JNTUA, Andhra Pradesh, India and working as an Associate professor in the department of Electronics and Communication Engineering, Aditya Engineering College, Surampalem, Andhra Pradesh, India.